Modelling and exergy analysis of a plasma furnace for aluminium melting process

Luis Acevedo[a], Sergio Usón[b], Javier Uche[c] and Patxi Rodríguez[d]

[a]*CIRCE-University of Zaragoza, Zaragoza, Spain, leag@unizar.es*
[b]*CIRCE-University of Zaragoza, Zaragoza, Spain, suson@unizar.es (CA)*
[c]*CIRCE-University of Zaragoza, Zaragoza, Spain, javiuche@unizar.es*
[d]*TECNALIA – Foundry unit, San Sebastián, Spain, patxi.rodriguez@tecnalia.com*

Abstract:

The use of new heating systems like thermal plasma may entail significant improvements in reducing the energy consumption in energy intensive industries as metal foundry sector. In present work, a secondary foundry of aluminium model with two different heating technologies (propane gas combustion and nitrogen plasma) is presented in order to predict its performance. The model was developed to simulate thermal behaviour of a cylindrical crucible furnace in which aluminium is melted. It estimates the temperature of the combustion chamber and the transient heating in furnace walls and aluminium during melting and preheating stages. Equations were solved numerically by means of MATLAB scripts. Energy analysis compared the furnace performance of alternative heating processes (gas fed burner versus plasma). Results showed that thermal plasma is more efficient than a conventional gas burner: specific energy consumption is 52.6% lower. Besides, exergy analysis pointed out that exergy losses are reduced in case of plasma torch since heating is directly oriented into the load (aluminium). The model was validated with a battery test on a pre-commercial pilot plant at Tecnalia facilities. Thus, it could reduce the cost of that industrial laboratory when new design parameters are tested.

Keywords:

Plasma furnace, Aluminium, Energy consumption, Exergy and Efficiency.

1. Introduction

Aluminium is the most abundant metal of the Earth crust. It possesses low density and the ability to resist corrosion. Aluminium industry formally started at 1886 after the discovery of electrolysis as the way to produce it from fused salts. Since that year, its use has grown rapidly and overtaken other metals, such as copper, tin and lead [1], and its cost steadily declined and engineering applications became economically viable [2]. Nowadays, it is the second most widely used metal after steel. Average energy consumption for producing primary aluminium is about 16500 kWh/ton, being the 5.5% (~908 kWh/ton) consumed for melting/casting. The average energy consumption for producing secondary aluminium (melting) is about the 6% of that required for primary aluminium [3].

1.1. Problem description

Industrial furnaces are insulated enclosures that are designed to deliver the heat required to process diverse loads [4]. Current melting furnaces used in the aluminium industry can be classified into three (heating) types: resistance, induction and gas- or oil-fired furnaces [5]. Major problem found during aluminium melting in conventional furnaces is the oxide formation and hydrogen absorption, which could affect the aluminium quality due to the oxide inclusions and higher porosity. As a very energy intensive process, the increasing limitation of raw materials for metallurgy processes, and the serious ecological problems involved, require not only to pay attention to reduce its use, but also in the technology used in its production. For instance, in [6] it was demonstrated that an improved conventional aluminium furnace with preheating and recirculation gas system reduces the fuel

consumption in 38%, while this work will show that fuel savings could reach to the 45% with plasma heating technology.

Main objective of the model is to predict the performance of a crucible heated up by two methods, as well as to calculate some temperature profiles that in practice are difficult to measure. Previous models [6-8] based their analysis on conventional gas burners. Alternatively, the use of plasma in thermal processing was described in [9-11] by means of the complete simulation of the plasma temperature profile and the support of Maxwell and Laplace equations. In [12], apart from the plasma temperature profiles, a complete heat transfer simulation was performed.

In this work, a conventional heating method was analysed and compared with a new heating system (plasma). The cornerstone of this article is to provide a flexible and reliable model that allows to predict the performance of the crucible upon diverse heating systems. To avoid thermal shock, aluminium furnace walls have to be preheated by a gas burner. Then, aluminium could be melted by two alternatives, propane combustion and plasma. The model requires as input data the next list:

- Energy: input energy used during preheating
- Walls and gases: convective and conductive heat transfer coefficients, and irradiative properties.
- Geometry and components of the furnace.
- Load: metal type and thermal properties.

Finally the results of both simulations were compared in order to analyse their efficiency.

1.2. General description of plasma

Thermal plasma is a mix of ions, electrons and neutral particles [13]. It is created by the ionization of a gas provoked by a sustained electric arc supplied between plasma cathode and anode. Elevated density of the electric field forms a high-speed plasma jet. Thermal plasma facilities operate with a D.C. power source. Two arc plasma types are normally found: non-transferred, in which plasma is contained between the cathode and a nozzle anode, and transferred arc type, in which the metallic load acts as the anode closing the circuit. Here, aluminium acts as the anode. Main components of plasma system are described in Fig. 1. Plasma system is fed with nitrogen, which is injected through the cathode.

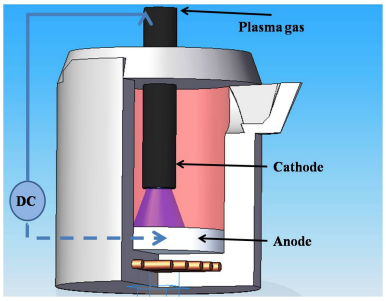

Fig. 1 Transferred arc plasma torch.

2. Furnace numerical simulation

2.1. Gas-fired preheating

Preheating was simulated by considering a high velocity propane gas burner. As it was pointed out by [7, 14], and due to the high recirculation inside of the crucible, a well-stirred model is assumed for combustion gases inside the furnace, and a 1-D model from the inside to outside of the furnace for aluminium load and refractory walls was used to simulate furnace.

The model adopted follows the previous analysis found in [7, 14, 15]. It consists of a governing equation for the combustion chamber, which is described in energy balance (1).

$$\rho \cdot V \cdot cp \cdot dT_g / dt = \dot{Q}_{hi} - \left\{ A_W \cdot \dot{q}_W + \dot{Q}_l + \dot{Q}_{stack} \right\} \quad (1)$$

Equation (1) is an ordinary differential equation that states that the heat provided by combustion gases is consumed in the stack and wall losses (*W*), as well as heating metal (*l*) for further melting. Initial condition for (1) depends on the heating process.

In order to calculate the radiative exchange in furnace, a grey-gas model was taken into account for exhaust gases coming from the burner. Procedure and properties of radiating gases can be found in [16-18]. Shape factors were computed for the furnace geometry distribution [19]. Representation of heat transfer modes can be found in Fig. 2.

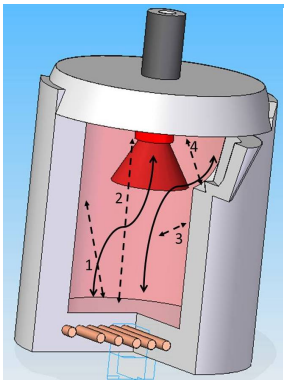

Line	Radiative transfer surfaces
1	wall ↔ bottom
2	cover ↔ bottom
3	wall ↔ wall
4	wall ↔ cover
solid lines	convection

Fig. 2 Heat transfer during preheating.

2.1.2. Computing the temperature profile of the furnace walls

Since its width is much smaller than its radius, walls were treated as a one slab governed by 1-D transient conduction equation:

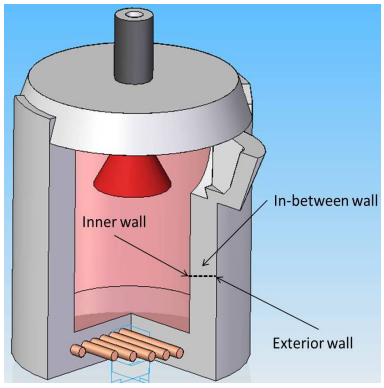

Fig. 3 One dimensional wall analysis.

$$\frac{\partial^2 T}{\partial x^2} + \frac{\dot{e}_{gen}}{k} = \frac{1}{\alpha}\frac{\partial T}{\partial t} \quad (2)$$

Boundary conditions for the walls are heat flux type, in which radiation and convection heat flows are calculated separately. At the beginning of the simulation (preheating stage) all surfaces are assumed to be at ambient temperature: at t=0, T_0=25ºC

$$-k\frac{\partial T}{\partial x} = \frac{\dot{Q}_{total}}{A} \quad (3)$$

$$\frac{\dot{Q}_{total}}{A} = J + \frac{\dot{Q}_{convection}}{A} \qquad (4)$$

Where J is the radiosity calculated following [18] and $Q_{convection}$ was computed following the procedure adopted in [7]. A FDM (finite difference method) was used to analyse and solve (2), by considering a differential wall element Δx. The energy balance on this element in a time interval Δt was expressed as in [7, 18, 20]. The finite difference formulation for an internal node can be expressed as:

$$T_{j-1}^{i} - 2T_{j}^{i} + T_{j+1}^{i} + \frac{\dot{e}_{j}^{i}\Delta x^{2}}{k} = \frac{T_{j}^{i+1} - T_{j}^{i}}{\tau} \qquad (5)$$

Spatial and temporal variations are represented by *j* and *i* respectively. Thermal diffusivity, time interval and differential wall element are related each other by the mesh Fourier number, τ:

$$\tau = \frac{\alpha\Delta t}{\Delta x^{2}} \qquad (6)$$

To complete the equations system of the FDM in refractory wall, equations on the boundary nodes are needed:

$$T_{0}^{i+1} = \left(1 - 2\tau - 2\tau\frac{h\Delta x}{k}\right)T_{0}^{i} + 2\tau T_{1}^{i} + 2\tau\frac{h\Delta x}{k}T_{\infty} + \tau\frac{\dot{e}_{0}^{i}\Delta x^{2}}{k} \qquad (7)$$

Once the system is completed and initial conditions are specified, the solution of transient problem is obtained by (5) and (7).

2.2. Aluminium melting with propane combustion

A 1-D conduction model was also used to estimate the aluminium temperature profile. Fig. 4 shows the new configuration inside of the furnace, as well as the temperature nodes inside of the aluminium layer studied here. Energy coming from exhaust gases or plasma increases the temperature in the upper node; then it is transferred energy by conduction to the lower nodes until the melting process finished.

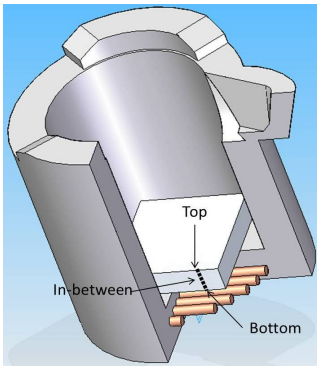

Fig. 4 Load configuration inside the furnace (during gas melting).

Similar equations than those used in refractory walls were implemented to simulate the aluminium melting process. Three different boundary conditions were implemented here:

- Sensible metal heating (liquid and solid): boundary heat flux conditions were defined.
- Phase change (latent heat): constant temperature was established.
- Aluminium in contact with the refractory of furnace bottom: an interface boundary condition was added to the process:

$$k_{Al} A \frac{T_{j-1} - T_j}{\Delta x} + k_{wall} A \frac{T_{j+1} - T_j}{\Delta x} = 0 \quad (8)$$

If aluminum is melted with the propane burner, similar equations are used with respect to preheating, only initial and boundary conditions are changed.

3. Aluminium melting with plasma

In plasma simulation, exhaust gases inside the furnace are almost insignificant and heating is produced by the plasma flame which drives directly into the aluminium. Therefore, gases do not participate in heat transferred by radiation. Plasma heat transferred was simulated with the aid of three consecutive approaches: first, the Elenbass-Heller equation is required to propose a system of equations in which the electric field, temperatures distribution and Joule effect are related [21]. Then, simplifications of a plasma model were taken into account from the Steenbeck and Raizer channel models ("positive column"). Finally, plasma heat transferred to the aluminium is calculated as it is proposed in [22]. Detailed mathematical models are shown below, and the software modules developed to solve the plasma heating process are shown in Fig.5.

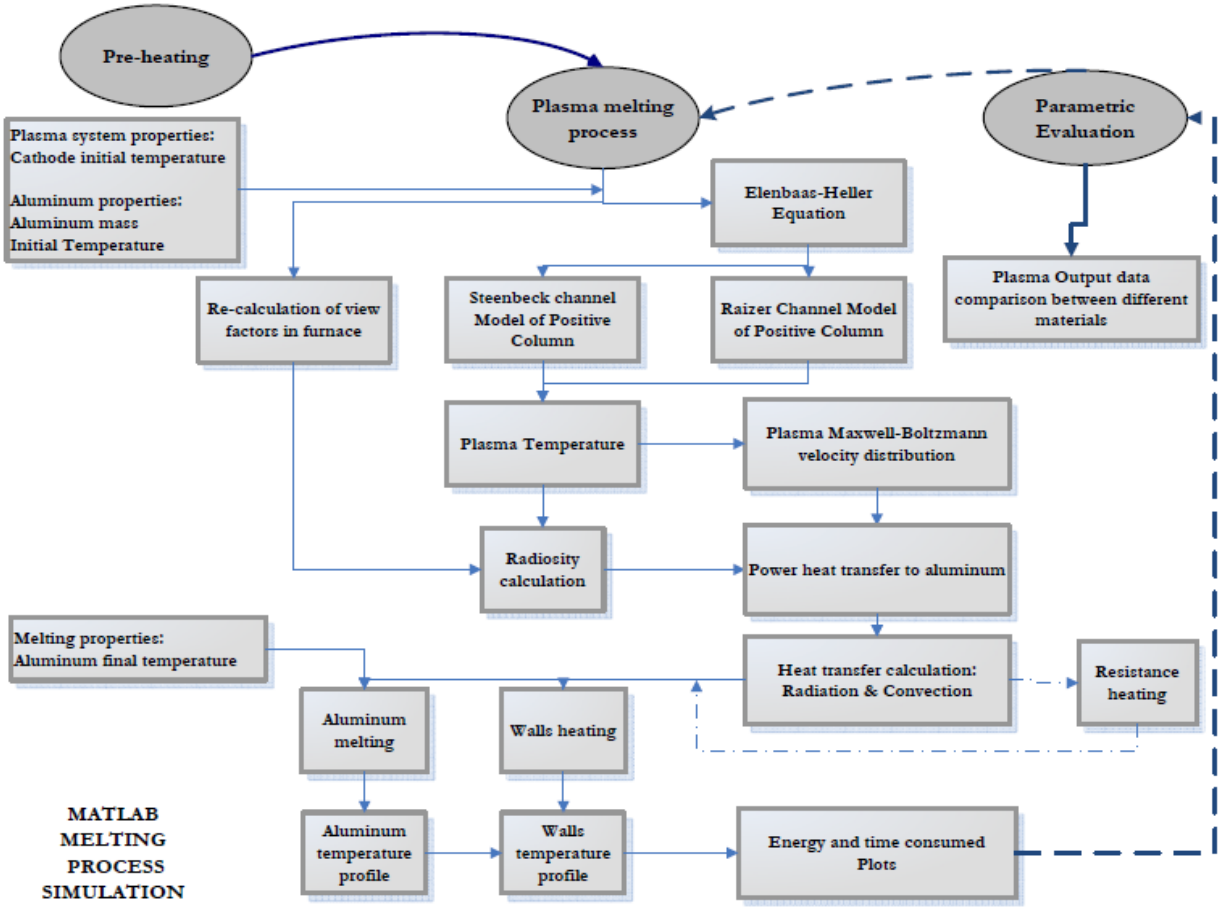

Fig. 5 Simulation architecture of plasma torch melting process.

When the aluminium melting is performed with plasma, the model takes into account several assumptions: it is considered that the current intensity during the whole process is kept constant, whereas the voltage (thus the power) varies (in order to maintain to the arc plasma stability). Radiosity is calculated as the radiant energy exchanged among the surfaces immersed in a transparent medium such as air, and anode effects are neglected. It was also considered that heat

transfer by convection was not relevant with respect to the radiation produced with plasma. Fig. 6 shows different surfaces involved during plasma melting process.

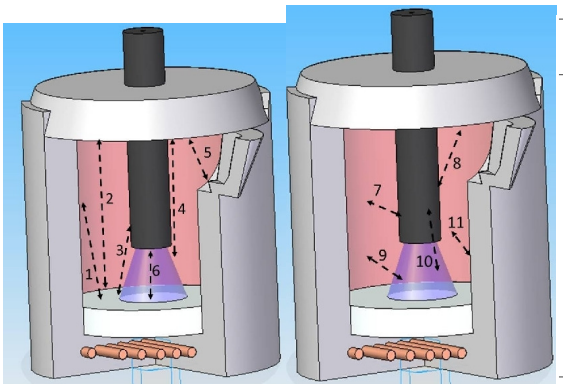

Line	Radiative transfer surfaces
1	wall ↔ aluminum
2	cover ↔ aluminum
3	cathode ↔ aluminum
4	plasma ↔ cover
5	wall ↔ cover
6	plasma ↔ aluminum
7	cathode ↔ wall
8	cathode ↔ cover
9	wall ↔ plasma
10	plasma ↔ cathode
11	wall ↔ wall

Fig. 6 Heat radiation transfer during plasma process

3.1. Simplified plasma equations

The description of the arc "positive column" model requires only the knowledge of the temperature distribution in plasma jet. Such distribution can be found from the Elenbaas-Heller equation [21]. In this equation, the gas pressure is considered a constant value, which is fixed by the experimental conditions:

$$\frac{1}{r}\frac{d}{dr}\left[r\lambda(T)\frac{dT}{dr}\right]+\sigma(T)E'^{2}=0 \qquad (9)$$

The above equation cannot be solved analytically because of the dependence of λ(T) and σ(T). For that reason, a simplified approach to the problem is required. The Steenbeck approach is based on the very strong exponential dependence of electric conductivity on the plasma temperature related in Saha equation [23], which explains the ionization expected in the plasma gas [21]. According to Steenbeck, temperature and electric conductivity can be considered as constant inside of the arc channel, and can be taken equal to their maximum value on the discharge axe. The total electric current of the arc can be expressed as:

$$I = E'\sigma\pi r_0^2 \qquad (10)$$

Application of this principle gives the additional equation of the Steenbeck model in the form that is required:

$$\left(\frac{d\sigma}{dT}\right)_{T=T_m}=\frac{4\pi\lambda\sigma}{w} \qquad (11)$$

To calculate the plasma flame temperature, the Raizer "Channel" Model of Positive Column was used. Key point of this model is the definition of an arc channel as a region where electric conductivity decreases not more than e times with respect to the maximum value at the discharge axe [21]:

$$\sigma(T)=83\exp\left(-\frac{36000}{T}\right) \qquad (12)$$

The electric field *E'* is kept constant along the positive column, so it actually describes the applied voltage.

$$E'=\frac{8\pi\lambda_m T_m^2}{I_i}\frac{1}{I} \qquad (13)$$

In (13) the ionization potential (I_i) is the energy required to remove electrons from gaseous atoms or ions, and the thermal conductivity of plasma jet (λ_m) is estimated constant (1.55 W/m-K), as found in [21, 24]. Thus, electric field is obtained from Steenbeck approach, and temperature was computed by using the Raizer model.

3.2. Plasma heat transfer model

In order to analyse the effect of plasma on the metal, it is necessary to firstly know the flow of plasma particles, and the number of particles per unit area and per unit time hitting the surface given by the product of normal speed to the metal surface [22].

$$v_z = v\cos\theta \tag{14}$$

The number of particles approaching the surface was taken into account and was described in a polar coordinate system as follows: for a small differential volume in velocity space between v and $v+dv$; and θ, and $\theta+d\theta$, ϕ and $\phi+d\phi$:

$$d\Gamma(v,\theta,\phi) = v_z dn(v,\theta,\phi) = \frac{v\cdot f'(v)\sin(\theta)\cos(\theta)d\phi d\theta dv}{4\pi} \tag{15}$$

$$\Gamma = n\left(\frac{2k'T}{\pi m'}\right)^{\frac{1}{2}}\int_0^\infty x^3 e^{-2x}dx = \frac{1}{4}n\left(\frac{8k'T}{\pi m'}\right)^{\frac{1}{2}} \tag{16}$$

In order to know the differential power flux [W/m^2], the differential particle flux must be multiplied by the kinetic energy of each particle.

$$dp(v,\theta,\phi) = \frac{1}{2}m'v^2 d\Gamma(v,\theta,\phi) \tag{17}$$

Substituting (16) in the above equation, the power heat transferred to the metal per unit area is finally obtained [22]:

$$p = \frac{m'}{8}\int_0^\infty v^3 f'(v)dv = \frac{nm'}{2\sqrt{\pi}}\left(\frac{2k'T}{m'}\right)^{3/2}\int_0^\infty x^5 e^{-x^2}dx \tag{18}$$

$$p = \frac{mn'}{2\sqrt{\pi}}\left(\frac{2k'T}{m'}\right)^{\frac{3}{2}} = 2k'T\Gamma \tag{19}$$

With (16), the plasma flow of particles was then computed, and (19) was used to calculate the plasma power delivered to aluminium. This power flux from plasma to the metal is the main parameter to obtain the temperature profile of aluminium. In this case, due to the high plasma temperature (above 8500 ºC) heat transfer by convection can be neglected.

To couple plasma and heat conduction models, equations from section 2.1.2 must be followed as well as boundary conditions from section 2.2. In order to define the link between plasma and heat transfer models, it is necessary to modify the boundary conditions (4).

$$\dot{Q}_{total,Al} = J + p \tag{20}$$

To compute the temperature profile in walls, only radiation was taken into account.

$$\dot{Q}_{total,walls} = J \tag{21}$$

4. Exergy balance of aluminium melting furnace

From previous simulation, mass and energy balances, as well as the furnace energetic efficiency were computed. However, in order to show which are the real potential savings in those complex

heating systems, it is necessary to perform an exergy analysis. The exergy flows are determined by the reference environment definition [25, 26].

The furnace is considered as a set of units consisting of container (made of refractory material) and different heating systems (gas burner or plasma torch). As it was explained before, there are also two heating stages to perform this melting process, see Fig. 7:

- Preheating: In this process, it can be distinguished two exergy inputs (fuel and air), three outputs (exergy of gas combustion, heat losses and the preheated refractory). The last one is not exactly an output flow, but it is considered the productive purpose of this heating stage.
- Aluminium melting: There are three exergy inputs, fuel (propane gas or electricity to activate plasma system), air in case of combustion (or nitrogen in case of plasma) and solid preheated aluminium. Exhausted gases (or ionized nitrogen), heat losses and liquid aluminium (as product) are the outputs of the system.

For a more detailed of exergy analysis, please refer to appendix A.

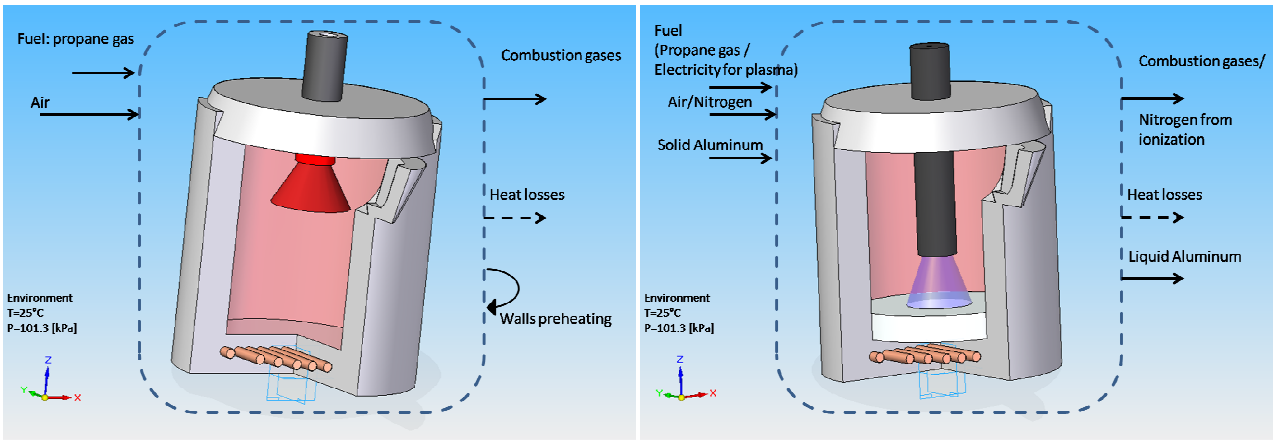

Fig. 7 Exergy balances for preheating (left) and melting (right)

5. Results and discussion

The model was validated with several experimental test performed at Tecnalia facilities. In each case, the temperature profile obtained at the end of the melting process and the energy consumption were compiled and then compared with those simulated. Fig. 8 shows energy consumption results for 5 tests with different aluminium loads and heating patterns: it can be seen that experimental data and simulated results were very similar, and both had the same specific energy ratio.

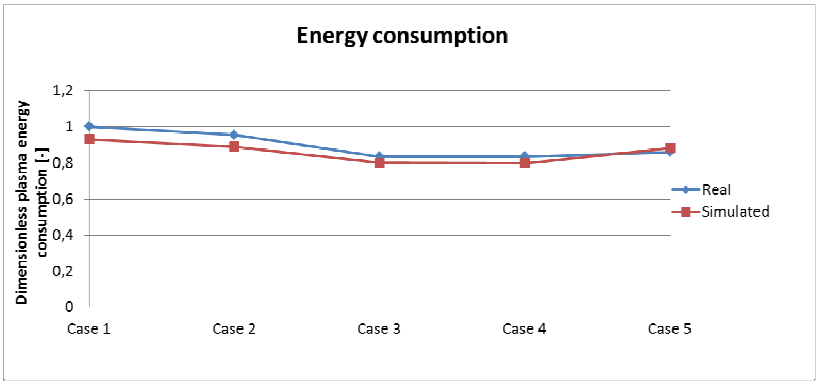

Fig. 8 Dimensionless experimental and simulated energy results

5.1. Energy analysis

Simulation was carried out on Matlab R2011a software. Results for a test including an aluminium load of 20.25 kg heated up to 760 ºC are shown in Table 1, which shows the comparison between the combustion and plasma results for melting. Energy efficiency of plasma without preheating is 67%, while energy consumption is about 0.46 kWh/kg and the furnace overall efficiency (melting and preheating) is 49.74%. Taking into account the energy consumed in the preheating process, the total specific energy consumed by the furnace is 0.95 kWh/kg. As expected, during the heating process, aluminium T-curve presents three different zones: first, temperature rises until the melting point. Here, the temperature is preserved until the energy from plasma equals the energy needed by the aluminium to be totally melted (at around 660ºC). Then, aluminium temperature continues rising until gets to a set-up temperature, as shown in Fig.9.a. Temperatures in furnace cover (T_{w3}) and walls (T_{w1}) are presented in Fig. 9.b: in almost 20 minutes of plasma melting, the temperatures inside the furnace walls get to 900 ºC.

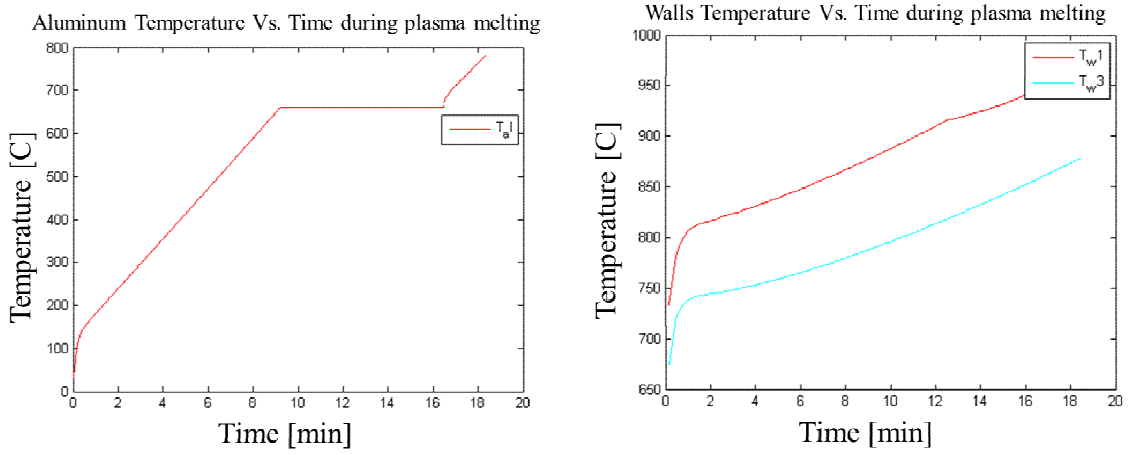

Fig. 9 Temperature evolution: a. Aluminium (left), b. furnace walls (rigth)

Table 1 simulation results for plasma and gas combustion

Parameter	Plasma simulation	Gas simulation	*Δ Plasma-Gas*
Furnace size, kg/h	40	40	0
Current intensity, A	600	-	-
Preheating gas power, kW	10	10	0
Melting power, kW	30	40	-10
Metal mass, kg	20.25	20.25	0
Final metal temp. C	782.63	769.09	13.05
Preheating time, min	60	60	0
Melting time, min	18.43	29.11	-10.68
Preheating energy, kWh	10	10	0
Melting energy, kWh	9.22	19.41	-10.19
Melting speed, kg/h	15.44	13.63	1.80
Melting efficiency, %	66.75	31.71	35.04
Furnace efficiency, %	49.74	32.26	17.47
Total specific energy, kWh/kg	0.95	1.45	-0.50

5.2. Exergy analysis

Annex A presents the main equations to solve exergy balance in the heating process. It can be observed in Table 2 that in plasma melting process, less irreversibilities are produced than in the case of propane gas combustion. For the same aluminium load, gas combustion during melting

consumes almost double of the exergy than in the case of plasma. Main reason is that in plasma furnace, exergy is emitted directly into the aluminium piece: at the end of the process, molten aluminium held the 51% of the input exergy. On the contrary, in propane combustion, heat is spread into walls and metal, therefore the exergy accumulated in molten aluminium is only the 23% of the input fossil fuel exergy. The same could be argued with respect to exergy destruction, in which gas fed furnace destroys three times the exergy destroyed with plasma.

Table 2 Exergy analysis

Parameter	Gas simulation	Gas simulation %	Plasma simulation	Plasma simulation %	Δ Plasma-Gas
Metal mass, kg	20.25		20.25		0
Fuel exergy, kWh	20.93	98.14	9.21	94.10	11.71
Initial metal exergy, kWh	0.5	1.86	0.5	5.9	0
Flue gas exergy, kWh	5.77	27.03	1.46	14.94	4.30
Exergy lost, kWh	1.6	7.51	1.09	11.23	0.50
Final metal exergy, kWh	5.07	23.75	5.07	51.78	0
Destroyed exergy during melting, kWh	8.89	41.70	2.09	21.42	6.79
Total fuel exergy (melting+preheating), kWh/kg	1.59	-	1.02		0.56
Total destroyed exergy, kWh/kg	0.76	-	0.43	-	0.32

5.3. Sensitivity analysis

The model could be also useful to analyze the variation of some design parameters in crucible furnaces. Then, a specific script was created to deal with thermal properties of refractories used in those furnaces. It is important to note that, independently of the heating mode, the highest energy consumption was found during the preheating.

First studied parameter was wall emissivity, often considered as an inherent physical property which usually remains unchanged. The emissivity of furnaces operating at high temperatures is usually about 0.3, but using high emissivity coatings can move to 0.8, thus reducing the fuel consumption by 25 to 45 per cent [27].

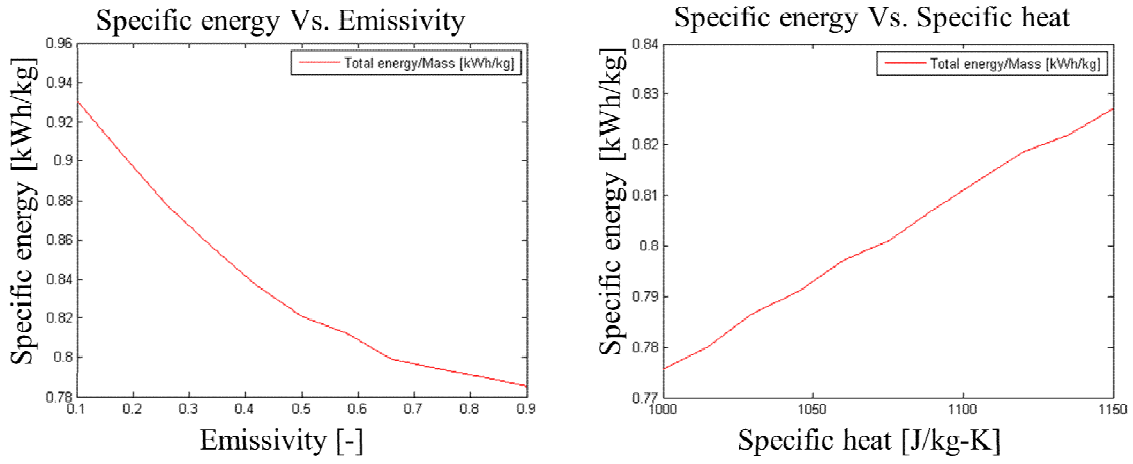

Fig. 10 Parametric simulations, energy consumed when: emissivity (left) and specific heat (right) is varied.

Figure 10 shows that this simulation (plasma case) exactly meets the behaviour described in literature: it can be observed a decrement of almost 30% of the energy consumption when the emissivity rises from 0.3 to 0.85.

Thermal capacity of refractory was also studied by varying the walls specific heat. As expected, the energy consumption mainly increases during the preheating as specific heat increases, because of the difficulty to obtain the desired temperature.

6. Conclusions

In this work, two heating modes for melting aluminium in a secondary crucible furnace were simulated. Both simulations (plasma and propane combustion) were developed in parallel with the aim of performing the automatic comparison. Simulation model was validated with experimental data taken from an industrial pilot plant. In the case of plasma, preheating (by means of a burner) represents the 52% of total energy consumed in the process (20.25 kg of aluminum were melted). In fact, this implies that energy savings can be mainly found in the preheating stage. On the other hand, exergy analysis fairly explained the reasons of the better plasma efficiency: if thermal shock problems are avoided in load and walls, plasma strongly reduces the energy consumption in the process. Taking into account that technical and economic constraints associated to experimental tests are found, it was proved that the model could help in its cost reduction of the design phase of those furnaces, since it is able to predict power consumption and provide some optimization guidelines. To test the feasibility of new heating systems, it could contribute to pave the way to reduce the energy intensity and their associated environmental impacts in this sector.

Appendix A

A.1. Exergy analysis

Considering the whole preheating and melting process, the overall exergy balance of a furnace is expressed as:

$$\sum B_{in} - \sum B_{out} = \sum B_{destroyed} \qquad \text{(A.1)}$$

The previous terms are defined in a different way in the case of preheating and melting.

- Preheating:

$$\sum B_{in} = B_{fuel} + B_{air} \qquad \text{(A.2)}$$

$$\sum B_{out} = B_{walls} + B_{gas} + B_{losses} \qquad \text{(A.3)}$$

- Melting:

$$\sum B_{in} = B_{fuel} + B_{air/N_2} + B_{solid\ Al} \qquad \text{(A.4)}$$

$$\sum B_{out} = B_{liquid\ Al} + B_{gas} + B_{losses} \qquad \text{(A.5)}$$

Where:

$$B_{walls} = m_{wall}\left(c_{wall}\left(T_{w,pre} - T_0\right) - T_0 c_{wall} \ln\frac{T_{wall,pre}}{T_0}\right) \qquad \text{(A.6)}$$

$$B_{gas,ph} = \sum_{i=1}^{nt} \dot{m}_{gas,i} \cdot \Delta t \left(c_{gas,i}\left(T_{gas,i} - T_0\right) - T_0 c_{gas,i} \ln\frac{T_{gas,i}}{T_0}\right) \qquad \text{(A.7)}$$

For each gas, the specific heat is calculated from [28]:

$$c_{gas,i} = a + b \cdot T_{gas,i} + c \cdot T_{gas,i}^2 + d \cdot T_{gas,i}^3 \qquad \text{(A.8)}$$

Since all chemical species of gases are presented in the reference environment, chemical exergy is calculated as in [29]:

$$B_{gas,ch} = \sum_{i=1}^{nt} \dot{m}_{gas,i} \Delta t \left[R_{gas,i} \cdot \sum_{k=1}^{ng} Y_{gas,i}^{k} T_0 \cdot \ln \frac{Y_{gas,i}^{k}}{Y_{0,gas}^{k}} \right] \qquad \text{(A.9)}$$

Total gas exergy is defined by:

$$B_{gas.tot} = B_{gas,ch} + B_{gas,ph} \qquad \text{(A.10)}$$

B_{losses} term represents all the heat losses in the system, this term cannot be computed directly:

$$B_{losses} = Q_{losses} \left(1 - \frac{T_0}{T_{ab}} \right) \qquad \text{(A.11)}$$

$$Q_{losses} = E_{fuel} - E_{product} - E_{gas} \qquad \text{(A.12)}$$

where T_{ab} is the average temperature of the control volume boundary. Equation (A.12) calculates losses from the overall balance of the furnace. In this equation, $E_{product}$ is defined depending on the heating process:

- Preheating: the product is the preheated refractory; $E_{product}$ is the energy stored in walls that avoids thermal shock. For this analysis (A.6) is computed.
- Melting: the product is the molten aluminium and exergy related to temperature variation in walls is included in the losses term. For this analysis, (A.6) is obviously not computed.

In order to compute exergy, it is necessary to firstly know the temperature of the process. This value was calculated as described in sections 2 and 3. Since it is considered that there are not chemical reactions during the melting process only thermo-mechanic exergy component is taken into account:

- Initial aluminium exergy value (during heating of solid aluminium):

$$B_{solid,Al} = m_{Al} \left(c_{Al,s} \left(T_{Al,i} - T_0 \right) - T_0 c_{Al,s} \ln \frac{T_{Al,i}}{T_0} \right) \qquad \text{(A.13)}$$

- Final aluminum exergy value, (during heating of liquid aluminium):

$$B_{liq,Al} = m_{Al} \left(c_{Al,l} \left(T_{Al,i} - T_f \right) - T_0 c_{Al,l} \ln \frac{T_{Al,i}}{T_f} \right) + B_{phasechange,Al} \qquad \text{(A.14)}$$

Where phase change exergy of aluminium is defined as:

$$B_{phasechange,Al} = m_{Al} \left(c_{Al,s} \left(T_{Al,f} - T_0 \right) - T_0 c_{Al,s} \ln \frac{T_{Al,f}}{T_0} \right) + Q_{phasechange} \cdot \Delta t \cdot \left(1 - \frac{T_0}{T_{Al,f}} \right) \qquad \text{(A.15)}$$

Acknowledgments

This work is part of the EDEFU project FP7-NMP-2009-LARGE3 with the grant agreement nº 246335. First author acknowledges the support from the Mexican *Consejo Nacional de Ciencia y Tecnología (CONACYT)* through the scholarship number 25712.

Nomenclature

Thermodynamic symbols

A area, m^2

B exergy, J

c specific heat, J/(kg K)

e internal heat generation, W/m^3

E energy, J

f friction factor

F shape factor

G absorbed energy, W/m^2

h heat transfer coefficient, $W/(m^2 K)$

J radiosity, W/m^2

k thermal conductivity, W/(m K)

k_g absorption coefficient, 1/(m-atm)

m mass, kg

$\dot{m}$ mass flow rate, kg/s

nt number of time steps

ng number of gas components

$\dot{q}$ heat per area, W/m^2

$\dot{Q}$ heat rate, W

Q heat, J

T temperature, K

t time, s

V volume, m^3

Y molar fraction

x differential element

Plasma symbols

E' electric field, V/m

$f'(v)$ maxwellian distribution

I electric current, A

I_i ionization potential, eV

k' Boltzmann constant, J/K

m' electron mass, kg

n density number, particles/m^3

p power flux, W/m^2

r radius, m

v particles velocity, m/s

w joule heat per length, W/m

Thermodynamic Greek symbols

α thermal diffusivity, m^2/s

η efficiency

ρ density, kg/m^3

τ mesh Fourier number

Plasma Greek symbols

Γ Plasma particle flux, particles/(m^2 s)

θ Plasma azimuthal angle

λ Plasma thermal conductivity, W/(m K)

σ Plasma electric conductivity, S/m

ϕ Plasma polar angle

Subscripts and superscripts

0 reference

1 furnace walls

3 furnace cover

ab average boundary

ch chemical

f melting point

g gas

hi fuel

i time interval

j node

k gas component

l Fusion energy

m plasma

ph physical

pr preheating

W *walls*

References

[1] Green, J. Aluminium recycling and processing for energy conservation and sustainability. USA: ASM International, 2007.

[2] Kaufman, J. and L., Elwin. Aluminium Alloy Castings: Properties, Processes, and Applications. USA: ASM International, 2004.

[3] Fu, M., Staples, K. and Sarvepalliis, V. A high-capacity melt furnace for reduced energy consumption and enhanced performance. JOM Journal of the Minerals, Metals and Materials Society, 1998;50(5):42-44.

[4] Trinks, W, et al. Industrial Furnaces, Sixth Edition. USA: John Wiley & Sons, Inc, 2004.

[5] Babos, L. and Martegani, A. D. Energy conservation and recovery in electric arc furnaces dedusting plants. Energy Conversion and Management, 1982;22(4):347-355.

[6] Lee, D. Exergy Analysis and efficiency evaluation for an aluminium melting furnace in a die casting plant [dissertation]. Totronto, Canada: Ryerson University; 2003.

[7] A., Ighodalo O. Development and performance evaluation of a melting furnace for non-ferrous metals. Internal Journal University Epoma-Nigeria, 2010;4:133-138.

[8] Hakan, C. and Arif, H. Exergetic analysis and assessment of industrial furnaces. Journal of Energy Resources Technology, ASME, 2010;132(1):(7 pages).

[9] Mimura K., Komukai T., and Isshiki M. Purification of chromium by hydrogen plasma-arc zone melting. Materials Science and Engineering A 2005;403(1-2):11-16.

[10] Mohebi M., Syedein S. and Reza M. Fluid flow and heat transfer modeling of AC arc in ferrosilicon submerged arc furnace. Journal of iron and steel research, international, 2010;17 (9):14-18.

[11] Wang H., Cheng K., Xhen X. and Pan W. Three dimensional modeling of heat transfer and fluid flow in laminar plasma material re-melting processing. International journal of heat and mass transfer, 2010;49(13-14):2254-2264.

[12] Chu S. and Lian S., Numerical analysis of temperature distribution of plasma arc with molten pool in plasma arc melting. Computational Materials Science, 2004;30(3-4):441-447.

[13] P.V., Ananthapadmanabhan, Venkatramani, N. and Suryanarayana, C. Thermal plasma processing, Pergamon Materials Series. 1999. p. 121-150.

[14] Bui, R. T. and Perron, J. Performance analysis of the Aluminium casting furnace. Metall. Trans. 1988;19(B):171-180.

[15] Davies, I. Master and Gethin, D. J. Numerical modeling of a rotary aluminium recycling furnace. 4th International symposium of recycling of metals and engineered materials.

[16] Tucker, R. J. Gas emissivity. Gas emissivity. 2003. <http://m.safe.mn/3gHI> [accesed 4.26.2011].

[17] Rhine, J. M. and Tucker, R. J. Modelling of gas-fired furnaces and boilers. McGraw-Hill; 1991.

[18] Holman. Heat transfer. McGraw-Hill; 1986.

[19] Howell, J. A catalog of radiation configuration factors. McGraw-Hill; 1982.

[20] Çengel. Heat and Mass transfer. McGraw-Hill; 2007.

[21] Fridman, A. and Kennedy, L. Plasma Physics and Engineering. Taylor and Francis; 2004.

[22] Reece, J. Industrial plasma engineering volume 1: principles.Taylor and Francis; 1995.

[23] Chen, F. Introduction to plasma physics and controlled fusion. Plenum press; 1984.

[24] Dunn, G. and Eagar, T. Calculation of Electrical and Thermal Conductivities of Metallurgical Plasmas. WRC Bulletin. 1990.

[25] Kotas, J. The exergy method of thermal plan analysis. Butterworths; 1985.

[26] Szargut, J. Exergy Method: Technical and Ecological Applications Developments in Heat Transfer, WITpress; 2005.

[27] Energy Efficiency Guide for Industry in Asia. Energy Efficiency Guide for Industry in Asia goverment. <www.energyefficiencyasia.org>[accessed 5.20.2011].

[28] Çengel, Y. A. and A., Boles M. Thermodynamics: An Engineering Approach. McGraw-Hill; 2006.

[29] Moran, M. J. and Shapiro, H. N. Fundamentals of engineering thermodynamics, 3rd ed. Wiley; 2000.